

# Phonon-Induced Zero-bias Currents in Solids

Masao OGATA<sup>1,2\*</sup> and Hidetoshi FUKUYAMA<sup>3</sup>

<sup>1</sup>*Department of Physics, University of Tokyo, Hongo, Bunkyo-ku, Tokyo 113-0033, Japan* <sup>2</sup>*Hongo 7-3-1, Bunkyo-ku, Tokyo 113-0033, Japan*

<sup>2</sup>*Research Institute for Energy Efficient Technologies, National Institute of Advanced Industrial Science and Technology (AIST), Umezono, Tsukuba, Ibaraki 305-8568, Japan*

<sup>3</sup>*Research Institute for Science and Technology, Tokyo University of Science, Shinjuku-ku, Tokyo 162-8601, Japan*

Zero-bias current induced by injected phonons in metals and one-dimensional charge density wave (CDW) systems attached on the surface of the piezoelectric substrate is investigated microscopically based on the second order response theory. In contrast to the shift currents discovered by von Baltz and Kraut in which the zero-bias current is induced by AC electric field in systems without inversion symmetry, propagating phonons break the inversion symmetry in the present case. The effects of both deformation potential and piezoelectric potential are taken into account. In the CDW system, zero-bias current appears below the transition temperature and its magnitude strongly depends on the position of the chemical potential. Possible experimental consequences are discussed.

## 1. Introduction

It is well-established that the existence of persistent current (zero-bias current) is a particular feature of superconductivity. Possibility of similar zero-bias currents has been predicted in insulators by von Baltz and Kraut in 1981 for systems without inversion symmetry under AC electric field<sup>1)</sup> followed by many experiments confirming the prediction. This important finding by von Baltz and Kraut of combined effects of second order external perturbations and inversion symmetry breaking has versatile consequences in condensed matter science.<sup>2)</sup> Experimentally, the zero-bias current should be observed in the current ( $I$ )-voltage( $V$ ) curve as shown in Fig. 1. It is to be noted that the zero-bias current in the present case is a dissipative current induced by external forces, in contrast to the non-dissipative persistent current in superconductivity.

The acoustoelectric effect is an effect in which zero-bias DC currents are induced by injected bulk acoustic phonons. This was first proposed by Parmenter,<sup>3)</sup> followed by some early experiments.<sup>4-7)</sup> In these cases, the zero-bias current flows even if the system has inversion symmetry because the finite propagating vector  $\mathbf{Q}$  of the acoustic phonon breaks the inversion symmetry. This acoustoelectric effect was analyzed in phenomenological theories,<sup>8-12)</sup> in which the attenuation of phonons results in electric current through the momentum transfer from phonons to electrons. However, in the presence of scattering of electrons by disorder, it is not clear how these phenomenological theories based on the momentum conservation law are valid. It is thus necessary to develop a microscopic theory using the second order nonlinear response.

Recently, acoustoelectric effects are studied experimentally in terms of surface acoustic waves (SAWs) or acoustic phonons propagating on the surface of a piezoelectric substrate. A zero-bias current is observed in graphene placed on

LiNbO<sub>3</sub>.<sup>13-21)</sup> Theoretically, Bhalla et al.<sup>22)</sup> developed a microscopic theory based on thermal Green's functions to study the case of graphene assuming that the SAW gives rise to the deformation potential, piezoelectric potential, and sound-induced vector potential<sup>23,24)</sup> on the two-dimensional electron system of graphene. [It is to be noted that the sound-induced vector potential is specific to the honeycomb lattice.<sup>23)</sup>] In the present paper, based on the microscopic method of Bhalla et al, we study the effects of SAW in metals in general. In particular, it is found by detailed analysis that this zero-bias current will have pronounced effects in the presence of CDW.

In section 2, we discuss the microscopic theory of the zero-bias current in terms of thermal Green's functions based on the second order response theory and apply the method to one-, two-, and three-dimensional metals. As the interaction between electron and phonon, we consider deformation potential and piezoelectric potential caused by the injected SAW. The obtained results show that the induced zero-bias current is proportional to the density of states multiplied by the momentum derivative of group velocity. In Section 3, we study the zero-bias current in one-dimensional CDW systems based on mean-field Hamiltonian. It is shown that the zero-bias current is induced below the transition temperature and its magnitude depends on the position of the chemical potential. In Section 4, we discuss possible experimental consequences.

## 2. Zero-bias current in metals

In this paper, we study electron systems interacting with an external propagating longitudinal acoustic (LA) phonon on the surface of substrate given by

$$\mathbf{u}(\mathbf{r}, t) = \mathbf{u}_0 \cos(\mathbf{Q} \cdot \mathbf{r} - \Omega t) = \frac{\mathbf{u}_0}{2} \left( e^{i\mathbf{Q} \cdot \mathbf{r}} e^{-i\Omega t} + e^{-i\mathbf{Q} \cdot \mathbf{r}} e^{i\Omega t} \right), \quad (2.1)$$

\*E-mail: ogata@hosi.phys.s.u-tokyo.ac.jp

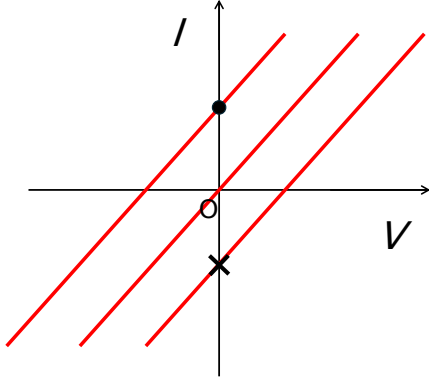


**Fig. 1.** (Color online) Schematic representation of  $I$ (current)- $V$ (voltage) curves in the presence of zero-bias currents together with ordinary Ohmic currents. Zero-bias current can be either plus (solid circle) for holes or minus (cross) for electrons at  $V = 0$ .  $V$  represents the voltage applied to the sample.

where we assume that the amplitude  $\mathbf{u}_0$  as a classical external field. First, we consider the situation in which the long-wavelength LA phonon induces local variation of average density of ions

$$\rho_i(\mathbf{r}) = \frac{\rho_i}{1 + \text{div } \mathbf{u}(\mathbf{r}, t)} \sim \rho_i(1 - \text{div } \mathbf{u}(\mathbf{r}, t)), \quad (2.2)$$

which leads to an external interaction Hamiltonian,  $H'$ , as in the electron-phonon interaction in metals. In addition, when the substrate is piezoelectric material, there is a piezoelectric potential.<sup>22, 25)</sup> Considering these two interactions, the external interaction Hamiltonian is given by

$$H'(t) = \sum_{\mathbf{k}, \sigma} [c_{\mathbf{k}+\mathbf{Q}, \sigma}^\dagger A_{\mathbf{Q}} c_{\mathbf{k}, \sigma} e^{-i\Omega t} + c_{\mathbf{k}-\mathbf{Q}, \sigma}^\dagger A_{-\mathbf{Q}} c_{\mathbf{k}, \sigma} e^{i\Omega t}], \quad (2.3)$$

where  $c_{\mathbf{k}, \sigma}$  and  $c_{\mathbf{k}, \sigma}^\dagger$  are the electron annihilation and creation operator and  $A_{\mathbf{Q}}$  is defined as

$$A_{\mathbf{Q}} = \frac{ig_1}{2} \mathbf{Q} \cdot \mathbf{u}_0 + \frac{1}{2} g_P u_0. \quad (2.4)$$

Here,  $g_1$  is the deformation potential and  $g_P$  represents the coupling constant for the piezoelectric potential. Note that the two effects can be treated together in the form of eq. (2.4).<sup>22, 25)</sup>

In the second order response theory with respect to the electron-phonon interaction  $H'(t)$  in eq. (2.3), the current density in the  $\mu$ -direction with momentum  $\mathbf{q}$

$$j_{\mathbf{q}, \mu} = -|e| \sum_{\mathbf{k}, \sigma} c_{\mathbf{k}-\frac{\mathbf{q}}{2}, \sigma}^\dagger v_{\mathbf{k}, \mu} c_{\mathbf{k}+\frac{\mathbf{q}}{2}, \sigma}, \quad (2.5)$$

is obtained from the analytic continuation of a response func-

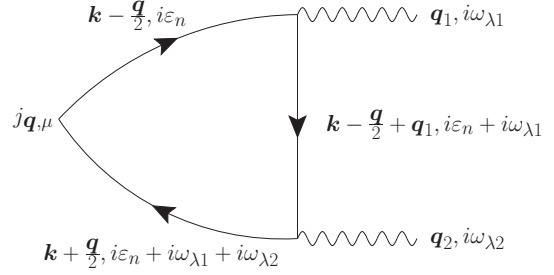


**Fig. 2.** Feynman diagram for the second order response theory. Solid lines represent thermal Green's functions and the wavy lines represent the perturbation  $H'(t)$ . The relation  $\mathbf{q} = \mathbf{q}_1 + \mathbf{q}_2$  has been noted. Note that the vertices associated with the perturbation have Matsubara frequencies  $i\omega_{\lambda 1}$  and  $i\omega_{\lambda 2}$  with  $\omega_{\lambda 1} > 0$  and  $\omega_{\lambda 2} > 0$ .

tion

$$\begin{aligned} \Phi_{\mathbf{q}}^{(2)}(i\omega_{\lambda 1}, i\omega_{\lambda 2}) &= -|e|k_B T \sum_n \sum_{\mathbf{k}, \sigma} \text{Tr} \left[ v_{\mathbf{k}, \mu} \mathcal{G} \left( \mathbf{k} - \frac{\mathbf{q}}{2} + \mathbf{q}_1 + \mathbf{q}_2, i\varepsilon_n + i\omega_{\lambda 1} + i\omega_{\lambda 2} \right) \right. \\ &\quad \left. \times A_{\mathbf{q}_2} \mathcal{G} \left( \mathbf{k} - \frac{\mathbf{q}}{2} + \mathbf{q}_1, i\varepsilon_n + i\omega_{\lambda 1} \right) A_{\mathbf{q}_1} \mathcal{G} \left( \mathbf{k} - \frac{\mathbf{q}}{2}, i\varepsilon_n \right) \right] \delta_{\mathbf{q}-\mathbf{q}_1-\mathbf{q}_2, \mathbf{0}}, \end{aligned} \quad (2.6)$$

where  $v_{\mathbf{k}, \mu}$  is the electron group velocity defined as  $v_{\mathbf{k}, \mu} = \partial H_{\mathbf{k}} / \hbar \partial k_{\mu}$ ,  $\mathcal{G}(\mathbf{k}, i\varepsilon_n) = [i\varepsilon_n + \mu - H_{\mathbf{k}}]^{-1}$  is the thermal Green's function of electrons,  $k_B$  is the Boltzmann constant, and the trace (Tr) is taken when the model has a matrix form. Figure 2 shows the Feynman diagram of the corresponding process where the solid lines represent the Green's function,  $\mathcal{G}$ , and the wavy lines represent the perturbation  $H'(t)$ . The same process has been studied by Bhalla et al for graphene.<sup>22)</sup> Note that the vertices associated with the perturbation have Matsubara frequency  $i\omega_{\lambda 1}$  and  $i\omega_{\lambda 2}$  with  $\omega_{\lambda 1} > 0$  and  $\omega_{\lambda 2} > 0$ , and the analytic continuation is taken as  $i\omega_{\lambda 1} \rightarrow \hbar\Omega_1 + i\delta$  and  $i\omega_{\lambda 2} \rightarrow \hbar\Omega_2 + i\delta$  irrespective of the signs of  $\Omega_1$  and  $\Omega_2$  of the external fields.<sup>22, 26, 27)</sup> This is because the perturbation by  $H'(t)$  is not internal but external and should be treated as adiabatic as in the case of shift current.<sup>1, 28)</sup>

For  $\mathbf{q}_1$ ,  $\mathbf{q}_2$ ,  $\omega_{\lambda 1}$ , and  $\omega_{\lambda 2}$  in Fig. 2, we consider the two cases

- (a)  $\mathbf{q}_1 = \mathbf{Q}, i\omega_{\lambda 1} \rightarrow \hbar\Omega + i\delta, \mathbf{q}_2 = -\mathbf{Q}, i\omega_{\lambda 2} \rightarrow -\hbar\Omega + i\delta,$
  - (b)  $\mathbf{q}_1 = -\mathbf{Q}, i\omega_{\lambda 1} \rightarrow -\hbar\Omega + i\delta, \mathbf{q}_2 = \mathbf{Q}, i\omega_{\lambda 2} \rightarrow \hbar\Omega + i\delta,$
- (2.7)

which lead to the expectation value of uniform DC current  $\langle j_{\mathbf{q}=\mathbf{0}, x} \rangle$  as follows after summation over the fermion Matsub-

ara frequency  $i\varepsilon_n$ .

$$\begin{aligned} \langle j_x \rangle = & 2|e| \sum_k \int \frac{d\varepsilon}{\pi} f(\varepsilon) \text{Tr} \left[ v_{k,x} \right. \\ & \times \left\{ G_R(\mathbf{k}, \varepsilon) A_{-\mathbf{Q}} G_R(\mathbf{k} + \mathbf{Q}, \varepsilon + \hbar\Omega) A_{\mathbf{Q}} [\text{Im} G_R(\mathbf{k}, \varepsilon)] \right. \\ & + G_R(\mathbf{k}, \varepsilon - \hbar\Omega) A_{-\mathbf{Q}} [\text{Im} G_R(\mathbf{k} + \mathbf{Q}, \varepsilon)] A_{\mathbf{Q}} G_A(\mathbf{k}, \varepsilon - \hbar\Omega) \\ & + [\text{Im} G_R(\mathbf{k}, \varepsilon)] A_{-\mathbf{Q}} G_A(\mathbf{k} + \mathbf{Q}, \varepsilon + \hbar\Omega) A_{\mathbf{Q}} G_A(\mathbf{k}, \varepsilon) \\ & \left. \left. + (\mathbf{Q} \rightarrow -\mathbf{Q}, \Omega \rightarrow -\Omega) \right\} \right], \end{aligned} \quad (2.8)$$

where  $f(\varepsilon)$  is the Fermi distribution function defined as  $f(\varepsilon) = 1/[e^{(\varepsilon-\mu)/k_B T} + 1]$ , the factor 2 comes from the spin summation, and  $(\mathbf{Q} \rightarrow -\mathbf{Q}, \Omega \rightarrow -\Omega)$  means the contribution with  $\mathbf{Q}$  and  $\Omega$  in the preceding terms being replaced by  $-\mathbf{Q}$  and  $-\Omega$ . In eq. (2.8),  $G_R(\mathbf{k}, \varepsilon)$  is the retarded Green's function,  $G_A(\mathbf{k}, \varepsilon) = G_R^\dagger(\mathbf{k}, \varepsilon)$  is the advanced Green's function, and  $\text{Im} G_R(\mathbf{k}, \varepsilon) = (G_R(\mathbf{k}, \varepsilon) - G_A(\mathbf{k}, \varepsilon))/2i$ .

To evaluate  $\langle j_x \rangle$  at finite  $\mathbf{Q}$ , we note that expansion with respect to  $\mathbf{Q}$  is allowed since the wave vector  $|\mathbf{Q}|$  of LA phonon is small compared with the characteristic wave vector of electrons. Therefore, we note

$$\begin{aligned} G_{R(A)}(\mathbf{k} + \mathbf{Q}, \varepsilon) = & G_{R(A)}(\mathbf{k}, \varepsilon) + G_{R(A)}(\mathbf{k}, \varepsilon) \mathbf{Q} \cdot \boldsymbol{\gamma}_k G_{R(A)}(\mathbf{k}, \varepsilon) \\ & + O(|\mathbf{Q}|^2), \end{aligned} \quad (2.9)$$

where  $\boldsymbol{\gamma}_k$  is defined as  $\boldsymbol{\gamma}_k = \hbar \mathbf{v}_k = \partial H_k / \partial \mathbf{k}$ , and we have used the relationship  $\partial G_{R(A)} / \partial \mathbf{k} = G_{R(A)} \boldsymbol{\gamma}_k G_{R(A)}$  that holds also in the case of matrix form. Furthermore, since the phonon frequency  $\Omega = v_s |\mathbf{Q}|$  ( $v_s$  is the sound velocity) is small compared with electronic energy,  $\langle j_x \rangle$  is given by the expansion with respect to  $\Omega$ . We find that  $\langle j_x \rangle$  vanishes when  $\Omega = 0$ . Therefore, in the lowest order of  $\Omega$ , we obtain

$$\begin{aligned} \langle j_x \rangle = & 2|e|\Omega \int \frac{d\varepsilon}{\pi} f'(\varepsilon) \sum_k \mathbf{Q} \text{Im Tr} \\ & \left[ \boldsymbol{\gamma}_{k,x} G_{RA-\mathbf{Q}} G_{R\boldsymbol{\gamma}_{k,x}} G_{RA\mathbf{Q}} G_A \right. \\ & \left. - \frac{1}{2} \boldsymbol{\gamma}_{k,x} G_{RA-\mathbf{Q}} G_{R\boldsymbol{\gamma}_{k,x}} G_{RA\mathbf{Q}} G_R + (\mathbf{Q} \rightarrow -\mathbf{Q}) \right], \end{aligned} \quad (2.10)$$

where we have used  $\mathbf{Q} = (Q, 0, 0)$  and  $v_{k,x} = \gamma_{k,x}/\hbar$ . In eq. (2.10),  $G_{R(A)}$  is the abbreviation of  $G_{R(A)}(\mathbf{k}, \varepsilon)$  and  $(\mathbf{Q} \rightarrow -\mathbf{Q})$  means the contribution with  $\mathbf{Q}$  in the preceding two terms being replaced by  $-\mathbf{Q}$ .

For the explicit summation over  $\mathbf{k}$ , we assume free electrons with isotropic effective mass  $m$  in each dimension  $d$  together with the damping  $\Gamma$  independent of energy and momentum,  $G_R(\mathbf{k}, \varepsilon) = 1/[\varepsilon + i\Gamma - \hbar^2 k^2/2m]$ , and  $G_A = G_R^*$ . Here we assume that electronic damping  $\Gamma$  large enough compared to phonon energy, i.e.  $\Gamma > \hbar\Omega = \hbar v_s |\mathbf{Q}|$  ( $\cong 10^{-6}$  eV in cases of interest). Then summations over  $\mathbf{k}$  in eq. (2.10) in each di-

mension can be performed as follows,

$$\begin{aligned} d = 1, \\ \frac{m^2 L}{4\hbar^4} \text{Re} \left[ -\frac{1}{\kappa_R^5} + \frac{i\hbar^2}{m\Gamma\kappa_R^3} + \frac{\hbar^4}{m^2\Gamma^2\kappa_R} + \frac{i\hbar^6}{2m^3\Gamma^3} (\kappa_R - \kappa_A) \right], \end{aligned} \quad (2.11)$$

$$\begin{aligned} d = 2, \\ \frac{m^2 L^2}{6\pi\hbar^4} \text{Im} \left[ -\frac{1}{\kappa_R^4} + \frac{3i\hbar^2}{2m\Gamma\kappa_R^2} + \frac{3i\hbar^4}{4m^2\Gamma^2} \left( \frac{\pi}{2} + \tan^{-1} \frac{\varepsilon}{\Gamma} \right) \right], \end{aligned} \quad (2.12)$$

$$\begin{aligned} d = 3, \\ \frac{m^2 L^3}{24\pi\hbar^4} \text{Re} \left[ \frac{1}{\kappa_R^3} - \frac{3i\hbar^2}{m\Gamma\kappa_R} + \frac{3\hbar^4\kappa_R}{m^2\Gamma^2} + \frac{i\hbar^6}{2m^3\Gamma^3} (\kappa_R^3 - \kappa_A^3) \right], \end{aligned} \quad (2.13)$$

where  $\kappa_R = \sqrt{2m(\varepsilon + i\Gamma)}/\hbar$  ( $\text{Im } \kappa_R > 0$ ) and  $\kappa_A = \sqrt{2m(\varepsilon - i\Gamma)}/\hbar$  ( $\text{Im } \kappa_A > 0$ ). Note that  $\kappa_A = -\kappa_R^*$ , so that  $\kappa_R - \kappa_A = \kappa_R + \kappa_R^*$  and  $\kappa_R^3 - \kappa_A^3 = \kappa_R^3 + (\kappa_R^*)^3$  are both real and the last terms in eqs. (2.11) and (2.13) do not contribute.

For  $\Gamma \ll \varepsilon_F$ , we see that the dominant contribution in  $\langle j_x \rangle$  is in the order of  $\varepsilon_F^2/\Gamma^2$  at low temperatures where  $f'(\varepsilon) \sim -\delta(\varepsilon - \varepsilon_F)$  holds. In this case, we obtain

$$\begin{aligned} d = 1, \quad \langle j_x \rangle = & -|e| \frac{Q\Omega\hbar|A_{\mathbf{Q}}|^2 L}{\pi\Gamma^2 \sqrt{2m\varepsilon_F}}, \\ d = 2, \quad \langle j_x \rangle = & -|e| \frac{Q\Omega|A_{\mathbf{Q}}|^2 L^2}{2\pi\Gamma^2}, \\ d = 3, \quad \langle j_x \rangle = & -|e| \frac{Q\Omega|A_{\mathbf{Q}}|^2 L^3 \sqrt{2m\varepsilon_F}}{2\pi^2\hbar\Gamma^2}, \end{aligned} \quad (2.14)$$

where  $|A_{\mathbf{Q}}|^2 = u_0^2(g_1^2 Q^2 + g_p^2)/4$ . We see that  $\langle j_x \rangle$  is proportional to the density of states in each dimension multiplied by the  $k_x$ -derivative of the group velocity  $v_k$ . An alternative derivation of eq. (2.14) is given in Appendix. The present result shows that the phonon-induced zero-bias currents appear even in simple metals.

### 3. Zero-bias current in one-dimensional CDW system

In the following, we study the case of a one-dimensional CDW system described by the Hamiltonian

$$H_k = \xi_k \sigma_z + \Delta \sigma_x, \quad (3.1)$$

interacting with external propagating LA phonon on the surface of substrate, as shown in eq. (2.1). Here,  $\sigma_x$  and  $\sigma_z$  are the  $2 \times 2$  Pauli matrices,  $\xi_k = v_F \hbar k$  with  $v_F$  being the Fermi velocity, and  $\Delta$  represents the CDW order parameter. For the right-going (left-going) electrons, the momentum  $k$  is measured from  $k_F$  ( $-k_F$ ). In this case,  $\boldsymbol{\gamma}_{k,x}$  is a matrix  $\boldsymbol{\gamma}_{k,x} = v_F \hbar \sigma_z$  and the Green's functions are

$$G_R = \frac{\varepsilon_+ + \xi_k \sigma_z + \Delta \sigma_x}{D_R}, \quad G_A = \frac{\varepsilon_- + \xi_k \sigma_z + \Delta \sigma_x}{D_A}, \quad (3.2)$$

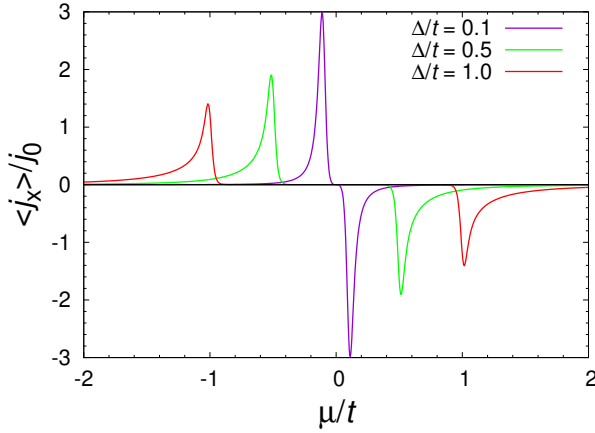


**Fig. 3.**  $\langle j_x \rangle / j_0$  as a function of  $\mu/t$  at  $T = 0$ , where  $j_0 = |e|Q\Omega v_F \hbar |A_Q|^2 L / (t\Gamma^2)$  with a unit of energy  $t$ .  $\Gamma$  is fixed at  $\Gamma/t = 0.05$  and  $\Delta$  are chosen as  $\Delta/t = 0.1, 0.5$  and  $1.0$ .

where  $\varepsilon_{\pm} = \varepsilon \pm i\Gamma$ ,  $D_R = \varepsilon_+^2 - \xi_k^2 - \Delta^2$  and  $D_A = (D_R)^*$ . Taking the trace in eq. (2.10), we obtain

$$\begin{aligned} \langle j_x \rangle &= 4|e|Q\Omega v_F^2 \hbar^2 |A_Q|^2 \int \frac{d\varepsilon}{\pi} f'(\varepsilon) \sum_k \\ &\times \text{Im} \left[ \frac{2}{D_R D_A} \left\{ 1 - \frac{2i\Gamma \varepsilon_+}{D_R} + \frac{8\xi_k^2}{D_R^2} \varepsilon \varepsilon_+ \right\} \right. \\ &\left. - \frac{1}{D_R^2} \left\{ 1 + \frac{8\xi_k^2}{D_R^2} \varepsilon_+^2 \right\} \right]. \end{aligned} \quad (3.3)$$

The summation over  $k$  results in

$$\begin{aligned} \langle j_x \rangle &= -|e|Q\Omega v_F \hbar |A_Q|^2 L \int \frac{d\varepsilon}{\pi} (-f'(\varepsilon)) \\ &\times \text{Re} \left[ \frac{\Delta^2}{\varepsilon^2 \Gamma^2 x_+} + \frac{i\Delta^2}{\varepsilon \Gamma x_+^3} - \frac{\Delta^2}{x_+^5} \right], \end{aligned} \quad (3.4)$$

with  $x_{\pm} = \sqrt{\varepsilon_{\pm}^2 - \Delta^2}$  ( $\text{Im}x_{\pm} > 0$ ). It is to be noted that the zero-bias current vanishes in the normal state with  $\Delta = 0$ . This seems to contradict the results in the previous section, where we have shown that the simple metals have zero-bias currents. However, it is not a contradiction because the present CDW model is special in the sense that the group velocity  $v_{k,x}$  is constant ( $v_{k,x} = \pm v_F$ ) and thus its  $k_x$ -derivative vanishes.

The  $\mu$ -dependence of  $\langle j_x \rangle$  at  $T = 0$  divided by  $j_0 = |e|Q\Omega v_F \hbar |A_Q|^2 L / (t\Gamma^2)$  is shown in Fig. 3 for  $\Gamma/t = 0.05$  and for several values of  $\Delta/t$ . Here, we choose  $t \equiv v_F \hbar / a$  as a unit of energy with  $a$  being the lattice constant. When  $\mu$  is positive (negative),  $\langle j_x \rangle < 0$  ( $\langle j_x \rangle > 0$ ), which means that the electrons (holes) are dragged by the surface acoustic phonon leading to a negative (positive) current. As seen from Fig. 3, there are peaks at  $\mu = \pm\Delta$  when  $\Delta$  is finite. In the case of  $\Gamma \ll |\mu| - \Delta$ , we see that the dominant contribution at  $T = 0$  comes from

the first term in eq. (3.4) proportional to  $\Gamma^{-2}$ , which gives

$$\langle j_x \rangle = -\frac{j_0 \Delta^2 t}{\pi \mu^2 \sqrt{\mu^2 - \Delta^2}} \theta(\mu^2 - \Delta^2) \text{sign} \mu. \quad (3.5)$$

This expression explains the behavior of  $\langle j_x \rangle$  in Fig. 3, i.e.,  $\langle j_x \rangle \propto -1/\mu^3$ , in the region  $|\mu| \gg \Delta$ . On the other hand, when  $\mu = \pm\Delta$ , the divergence in eq. (3.5) is suppressed by the presence of  $\Gamma$ . In this case, the dominant contribution at  $\mu = \pm\Delta$  turns out to be

$$\langle j_x \rangle = \mp \frac{7t}{8\pi \sqrt{\Gamma \Delta}} j_0, \quad (3.6)$$

where we have used  $x_{\pm} = \sqrt{\pm 2i\Gamma \Delta - \Gamma^2}$  when  $\mu = \pm\Delta$ , and  $x_{\pm} \sim (\pm 1 + i) \sqrt{\Gamma \Delta}$  in the limit of  $\Gamma \ll \Delta$ . The peak value of  $\langle j_x \rangle$  at  $\mu = \pm\Delta$  becomes smaller as  $\Delta$  becomes larger as seen in Fig. 3, which is consistent with the  $\Delta$ -dependence of the right-hand side of eq. (3.6).

To discuss the temperature dependence of  $\langle j_x \rangle$ , we consider the mean-field theory of the CDW state with the Hamiltonian  $H_k + \frac{K}{2} \Delta^2$ , where the second term represents the elastic energy loss due to the CDW order parameter. The self-consistency equation for  $\Delta$  becomes

$$\begin{aligned} K\Delta &= 2 \sum_k \frac{\Delta}{E_k} (1 - 2f(E_k)) \\ &= \frac{1}{\pi v_F \hbar} \int_{-t}^t d\xi \frac{\Delta}{E_{\xi}} (1 - 2f(E_{\xi})), \end{aligned} \quad (3.7)$$

where the factor 2 in the first line comes from the spin summation, in the second line  $E_{\xi} = \sqrt{\xi^2 + \Delta^2}$ , and a cut-off energy is assumed to be  $\pm t$ . Instead of solving eq. (3.7), we assume that the order parameter has a temperature dependence

$$\Delta(T) = \Delta_0 \tanh \left[ \frac{\pi k_B T_c}{\Delta_0} \sqrt{\frac{8}{7\zeta(3)} \frac{T_c - T}{T}} \right], \quad (3.8)$$

between  $0 < T \leq T_c$ , where  $\zeta(3)$  is the Riemann zeta function,  $\Delta_0$  is the CDW order parameter at  $T = 0$  ( $\Delta_0 = 2te^{-\pi v_F \hbar K/2}$ ), and the phase transition temperature is  $k_B T_c = \frac{\gamma}{\pi} \Delta_0 = 0.567 \Delta_0$  with  $\gamma$  being Euler's constant ( $\gamma \sim 0.577$ ). Using the form of  $\Delta(T)$  in eq. (3.8), we obtain temperature dependence of  $\langle j_x \rangle$  by

$$\begin{aligned} \langle j_x \rangle &= -|e|Q\Omega v_F \hbar |A_Q|^2 L \int \frac{d\varepsilon}{\pi} (-f'(\varepsilon)) \\ &\times \text{Re} \left[ \frac{\Delta(T)^2}{\varepsilon^2 \Gamma^2 x_+} + \frac{i\Delta(T)^2}{\varepsilon \Gamma x_+^3} - \frac{\Delta(T)^2}{x_+^5} \right]. \end{aligned} \quad (3.9)$$

When we consider a single-band model described by the Hamiltonian (3.1), there is an electron-hole symmetry and the chemical potential is fixed at  $\mu = 0$ . In this case, the zero-bias current is not induced since both the electrons and holes are equally dragged. However, in some materials, other overlapping bands exist near the Fermi energy in addition to the one-dimensional CDW system. In such cases, the chemical potential deviates from  $\mu = 0$ . When  $\mu > 0$  ( $\mu < 0$ ), the elec-

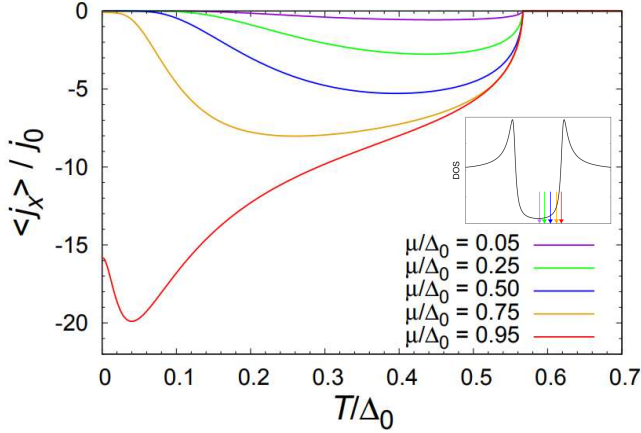


**Fig. 4.**  $\langle j_x \rangle / j_0$  as a function of temperature for several values of the chemical potential  $\mu$ . [ $\mu/\Delta_0 = 0.05, 0.25, 0.50, 0.75$ , and  $0.95$  from top to bottom.] The unit of energy is taken as  $\Delta_0$  that is the magnitude of the gap at  $T = 0$ .  $\Gamma$  is fixed at  $\Gamma/\Delta_0 = 0.10$ . The inset shows the positions of the chemical potentials.

trons (holes) are thermally excited more than the holes (electrons), leading to a negative (positive) induced current. Taking account of this possibility of nonzero- $\mu$ , we calculate the temperature dependence of  $\langle j_x \rangle$  for several values of the chemical potential as shown in Fig. 4 using the temperature dependence of  $\Delta(T)$  with  $\Delta_0 = 0.02t$ . The inset of Fig. 4 shows the positions of the chosen chemical potentials. Here, we use  $\Delta_0$  as a unit of energy and thus the phase transition temperature is  $T_c = 0.567\Delta_0/k_B$ . When the temperature is lowered below  $T_c$ ,  $\Delta(T)$  starts to develop and the induced current appears sharply. As the temperature decreases further, the gap  $\Delta(T)$  increases while the derivative of the Fermi distribution function ( $-f'(\varepsilon)$ ) becomes narrower as a function of  $\varepsilon$ . Combination of these two effects reduces the induced current at low temperatures. When  $\mu$  is close to zero, the absolute value of  $\langle j_x \rangle$  is small because of the cancellation between the contributions from electrons and holes. In contrast, when  $\mu$  is located close to the band edge ( $\mu \sim \pm\Delta_0$ ), the absolute value of  $\langle j_x \rangle$  remains large up to near zero temperature because  $\langle j_x \rangle$  has sharp peaks at the edge of the gap as shown in Fig. 3.

#### 4. Possible experimental consequences and summary

NbSe<sub>3</sub> is a candidate material of the one-dimensional CDW systems for observing the zero-bias current induced by SAW.<sup>29)</sup> As indicated by the resistivity experiment,<sup>30)</sup> NbSe<sub>3</sub> shows metallic behavior even below the two successive phase transition temperatures ( $T_1 = 140\text{K}$  and  $T_2 = 60\text{K}$ ) accompanied by enhancement of resistivity just below  $T_1$  and  $T_2$ . This means that there are other overlapping bands in addition to the CDW system. Therefore, the present results in Fig. 4 will be helpful for the analysis of temperature dependence of zero-bias current observed experimentally. Furthermore, from

the sign of the zero-bias current, we obtain the information whether the carriers are electron-like or hole-like. If the sign is negative (positive), the carriers are electrons (holes) irrespective of the sign of  $g_1$  and  $g_P$ .

To understand the experimental results quantitatively, it is necessary to evaluate the values of the coupling constants  $g_1$  and  $g_P$ , although they are not known experimentally. Nevertheless, by studying the  $Q$ -dependence of induced current, we will be able to obtain the information whether the zero-bias current originates from the deformation potential or not, because the contribution from  $g_1$  in  $\langle j_x \rangle$  is proportional to  $Q^3\Omega = v_s Q^4$ , while that from  $g_P$  is proportional to  $Q\Omega = v_s Q^2$  as shown in eq. (3.4). [Note that, in  $|A_Q|^2 = u_0^2(g_1^2 Q^2 + g_P^2)/4$ , the first term  $g_1^2 Q^2$  comes from the deformation potential and the second term  $g_P^2$  comes from the piezoelectric potential.]

For a rough estimate of the magnitude of the zero-bias current, we assume that  $u_0 g_P = 1$  meV and  $u_0 g_1 Q = 1$  meV tentatively. The other parameters are assumed to be  $Q = 6 \times 10^5$  m<sup>-1</sup>,  $v_F = 10^6$  m/sec,  $\Gamma = 2$  meV, and  $t = 1$  eV. The frequency of SAW is set to be 300 MHz, which corresponds to  $\Omega = 1.88 \times 10^9$  sec<sup>-1</sup>. When the cross-section of the CDW sample is  $10\mu\text{m} \times 0.04\mu\text{m}$  and the distance between the chains is 1 nm, we obtain  $j_0 \sim 10\text{nA}$ .

Let us discuss the relationship between our results of zero-bias current and those obtained phenomenologically. In the phenomenological theory, acoustoelectric current is given by<sup>8, 11, 12)</sup>

$$j_{\text{AE}} = -\frac{\alpha S \mu_e}{v_s}, \quad (4.1)$$

where  $\alpha$  is the sound attenuation,  $S$  is the power flux density of phonons, and  $\mu_e$  is the mobility of electrons. Here, the complete momentum transfer from phonon to electrons is assumed. However, in realistic cases with disorder, such as impurities, phenomenological considerations based on momentum conservation are not valid, because the momentum transferred to the electron system will decay owing to the disorder. Hence, there is no relationship between the phenomenological results and ours based on microscopic consideration under the assumption of  $\hbar\Omega = \hbar v_s Q < \Gamma$ .

To summarize, we have demonstrated that SAW induces zero-bias currents in metal in general. This is similar to the current discovered by von Baltz and Kraut for insulators without inversion symmetry under AC electric fields,<sup>1)</sup> in the sense that SAW plays roles of symmetry breaking in the present case of metals. Present theoretical results can be tested by experiments especially in NbSe<sub>3</sub>.

#### Acknowledgments

We thank very fruitful discussions with N. Nikaïdo, T. Kawada, M. Hayashi, K. Kitayama, and Y. Niimi. This work is supported by Grants-in-Aid for Scientific Research from the Japan Society for the Promotion of Science (No. JP23K03274 and No. JP23H01118), and JST-Mirai Program Grant (No. JPMJMI19A1).

### Appendix: Zero-bias current of single-band models in the small $\Gamma$ limit

In this appendix, we show that the zero-bias current  $\langle j_x \rangle$  of single-band models is proportional to the density of states multiplied by the  $k_x$ -derivative of the group velocity  $v_k$  in the limit of  $\Gamma \ll \varepsilon_F$ . In this limit, the dominant contribution to  $\langle j_x \rangle$  comes from the first term in eq. (2.10), which contains both the retarded ( $G_R$ ) and advanced ( $G_A$ ) Green's functions. In the single-band models with energy dispersion  $\varepsilon_k$ ,

$$\langle j_x \rangle = -2i|e|Q\Omega\hbar^2|A_Q|^2 \int \frac{d\varepsilon}{\pi} f'(\varepsilon) \sum_k v_{k,x}^2 \left\{ \frac{1}{(\varepsilon - \varepsilon_k + i\Gamma)^3 (\varepsilon - \varepsilon_k - i\Gamma)} - \frac{1}{(\varepsilon - \varepsilon_k + i\Gamma)(\varepsilon - \varepsilon_k - i\Gamma)^3} \right\}, \quad (\text{A}\cdot 1)$$

where we have used  $\gamma_{k,x} = \hbar v_{k,x}$  with  $v_{k,x} = \partial\varepsilon_k/\hbar\partial k_x$ . In the limit of  $\Gamma \ll \varepsilon_F$ , the dominant contribution is obtained from the residues of the poles of the Green's functions.<sup>31)</sup> Therefore, we obtain

$$\langle j_x \rangle = 4|e|Q\Omega\hbar^2|A_Q|^2 \sum_k \frac{v_{k,x}^2 f''(\varepsilon_k)}{(2i\Gamma)^2} + O(\Gamma^0). \quad (\text{A}\cdot 2)$$

Using the relation  $\hbar v_{k,x} f''(\varepsilon_k) = \partial f'(\varepsilon_k)/\partial k_x$ , we can perform the integration by part in the integral with respect to  $\mathbf{k}$ . As a result, the zero-bias current becomes

$$\langle j_x \rangle = |e| \frac{Q\Omega\hbar}{\Gamma^2} |A_Q|^2 \sum_k \frac{\partial v_{k,x}}{\partial k_x} f'(\varepsilon_k) + O(\Gamma^0). \quad (\text{A}\cdot 3)$$

The right-hand side is proportional to the density of states multiplied by the  $k_x$ -derivative of the group velocity. In the simple model with  $\varepsilon_k = \hbar^2 k^2/2m$ , we reproduce the results in eq. (2.14).

- 17) S. Zheng, H. Zhang, Z. Feng, Y. Yu, R. Zhang, C. Sun, J. Liu, X. Duan, W. Pang, and D. Zhang: *Applied Physics Letters* **109** (2016) 183110.
- 18) A. Hernández-Mínguez, Y.-T. Liou, and P. V. Santos: *Journal of Physics D: Applied Physics* **51** (2018) 383001.
- 19) J. R. Lane, L. Zhang, M. A. Khasawneh, B. N. Zhou, E. A. Henriksen, and J. Pollanen: *Journal of Applied Physics* **124** (2018) 194302.
- 20) P. Zhao, C. H. Sharma, R. Liang, C. Glasenapp, L. Mourokh, V. M. Kovalev, P. Huber, M. Prada, L. Tiemann, and R. H. Blick: *Phys. Rev. Lett.* **128** (2022) 256601.
- 21) Y. Mou, H. Chen, J. Liu, Q. Lan, J. Wang, C. Zhang, Y. Wang, J. Gu, T. Zhao, X. Jiang, W. Shi, and C. Zhang: *Nano Letters* **24** (2024) 4625.
- 22) P. Bhalla, G. Vignale, and H. Rostami: *Phys. Rev. B* **105** (2022) 125407.
- 23) H. Suzuura and T. Ando: *Phys. Rev. B* **65** (2002) 235412.
- 24) M. Vozmediano, M. Katsnelson, and F. Guinea: *Physics Reports* **496** (2010) 109.
- 25) G. D. Mahan: *Many-Particle Physics* (Springer Science+Business Media, New York, 2000).
- 26) R. Kubo: *Journal of the Physical Society of Japan* **12** (1957) 570.
- 27) A. D. Fetter and J. D. Walecka: *Quantum Theory of Many-Particle Systems*, pp. 302 (McGraw-Hill Book Company, New York, 1971).
- 28) J. E. Sipe and A. I. Shkrebtii: *Phys. Rev. B* **61** (2000) 5337.
- 29) N. Nikaïdo, T. Kawada, K. Fujiwara, N. Jiang, K. Kondou, S. Takada, and Y. Niimi: *private communication* (2026).
- 30) R. S. Lear, M. J. Skove, E. P. Stillwell, and J. W. Brill: *Phys. Rev. B* **29** (1984) 5656.
- 31) V. Könye and M. Ogata: *Phys. Rev. Res.* **3** (2021) 033076.

- 
- 1) R. von Baltz and W. Kraut: *Phys. Rev. B* **23** (1981) 5590.
  - 2) A. K. Jena, A. Kulkarni, and T. Miyasaka: *Chemical Reviews* **119** (2019) 3036.
  - 3) R. H. Parmenter: *Phys. Rev.* **89** (1953) 990.
  - 4) G. Weinreich and H. G. White: *Phys. Rev.* **106** (1957) 1104.
  - 5) W. Sasaki and E. Yoshida: *Journal of the Physical Society of Japan* **12** (1957) 979A.
  - 6) W.-C. Wang: *Phys. Rev. Lett.* **9** (1962) 443.
  - 7) J. R. A. Beale and M. Pomerantz: *Phys. Rev. Lett.* **13** (1964) 198.
  - 8) G. Weinreich: *Phys. Rev.* **107** (1957) 317.
  - 9) A. R. Hutson and D. L. White: *Journal of Applied Physics* **33** (1962) 40.
  - 10) K. A. Ingebrigtsen: *Journal of Applied Physics* **40** (1969) 2681.
  - 11) K. A. Ingebrigtsen: *Journal of Applied Physics* **41** (1970) 454.
  - 12) A. Wixforth, J. Scriba, M. Wassermeier, J. P. Kotthaus, G. Weimann, and W. Schlapp: *Phys. Rev. B* **40** (1989) 7874.
  - 13) V. Miseikis, J. E. Cunningham, K. Saeed, R. O'Rorke, and A. G. Davies: *Applied Physics Letters* **100** (2012) 133105.
  - 14) L. Bandhu, L. M. Lawton, and G. R. Nash: *Applied Physics Letters* **103** (2013) 133101.
  - 15) L. Bandhu and G. R. Nash: *Applied Physics Letters* **105** (2014) 263106.
  - 16) L. Bandhu and G. R. Nash: *Nano Research* **9** (2016) 685.